Supplementary Information

Highly Mesoporous Fe and N Co-doped Graphitic Catalysts Prepared from Short-time Synthesis of Precursor towards Highly Efficient Oxygen Reduction

Zu Zhong Gan, Zhao Min Sheng, Huan Huang, Xian You Dai, Rui Liang Niu and Run Ping Jia**

Experimental section

For the rotating ring-disk electrode (RRDE) experiments, the Fe-N_x-C slurry was coated on a GC ring-disk electrode with 1.5 μg mm^{-2}, and the 20% Pt/C catalyst (which is stocked from Johnson Matthey (JM) Co.) was loaded with 0.5 μg mm^{-2}. In addition, the ring electrode with a fixed potential was set on 0.5 V with a rotating speed at 1600 rpm.

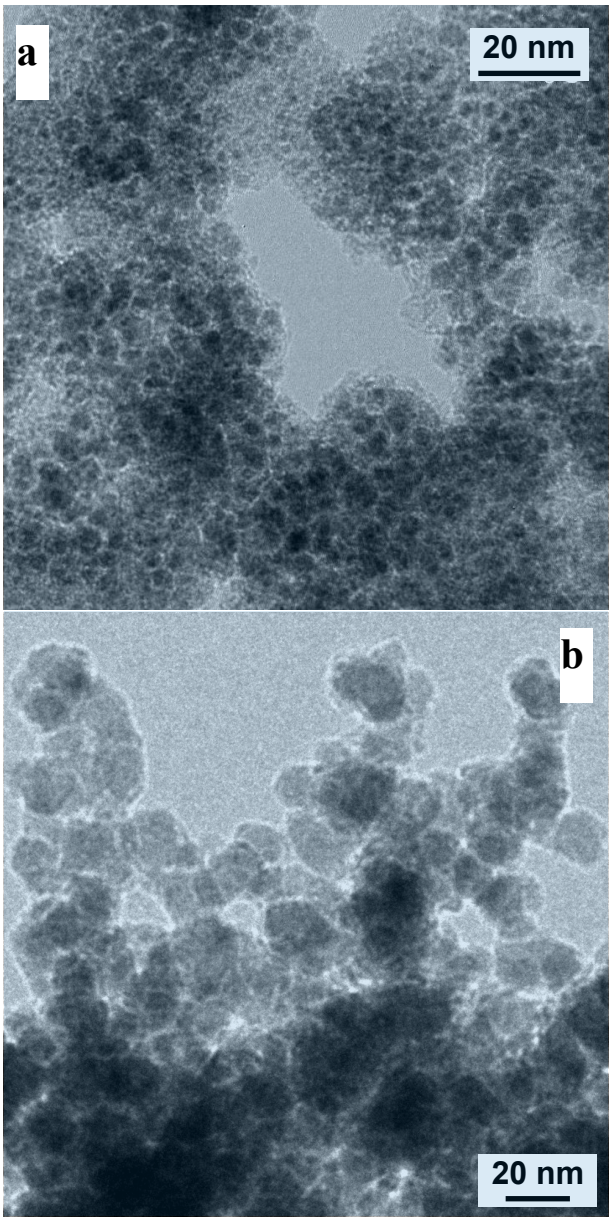

Fig. S1 TEM images of core-shell precursors: (a) Fe_3C@NDC700 and (b) Fe_3C@NDC1100.

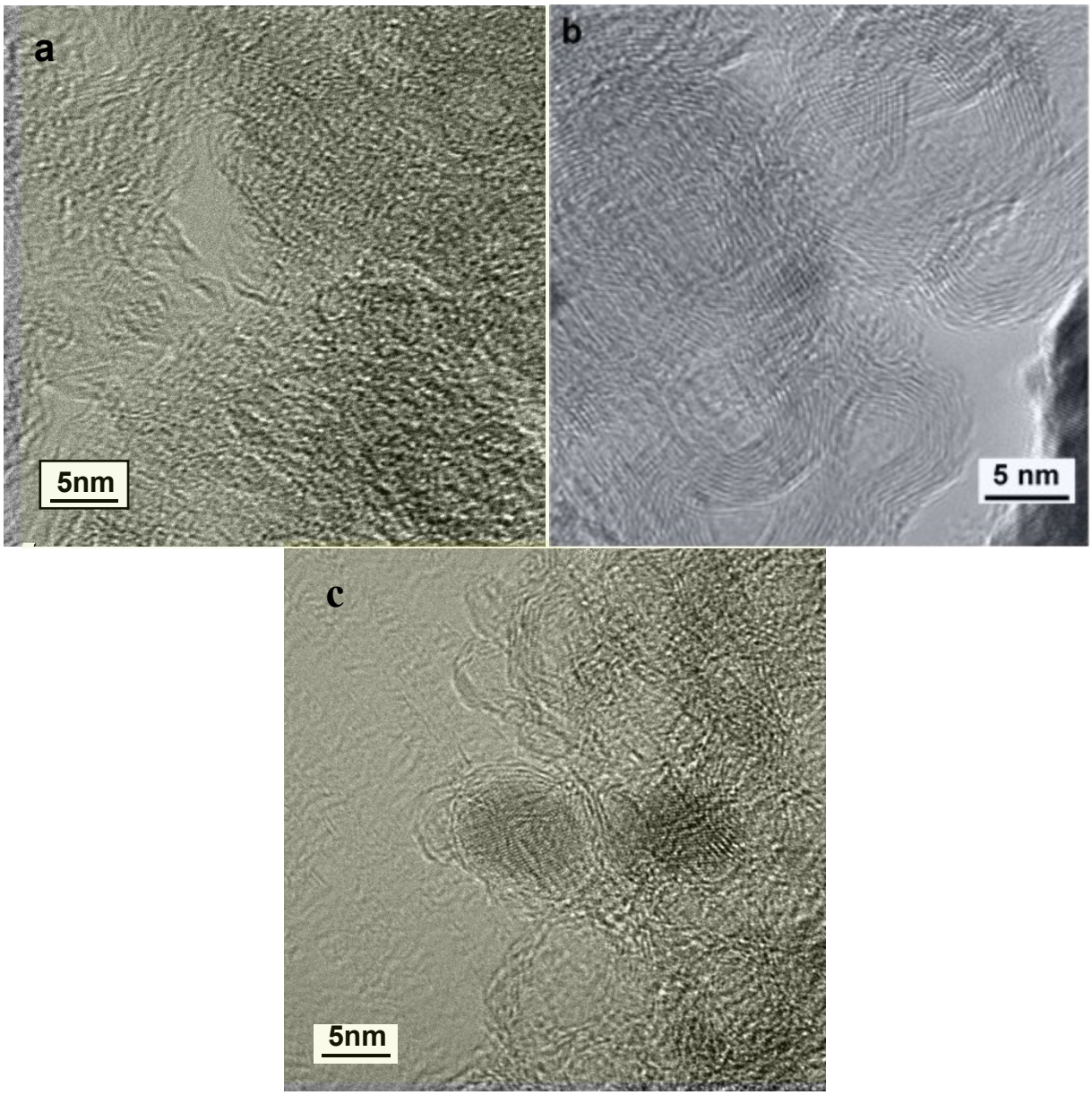

Fig. S2 HRTEM images of (a) Fe-N_x-C700, (b) Fe-N_x-C1100, (c) Fe-N_x-C900HCl.

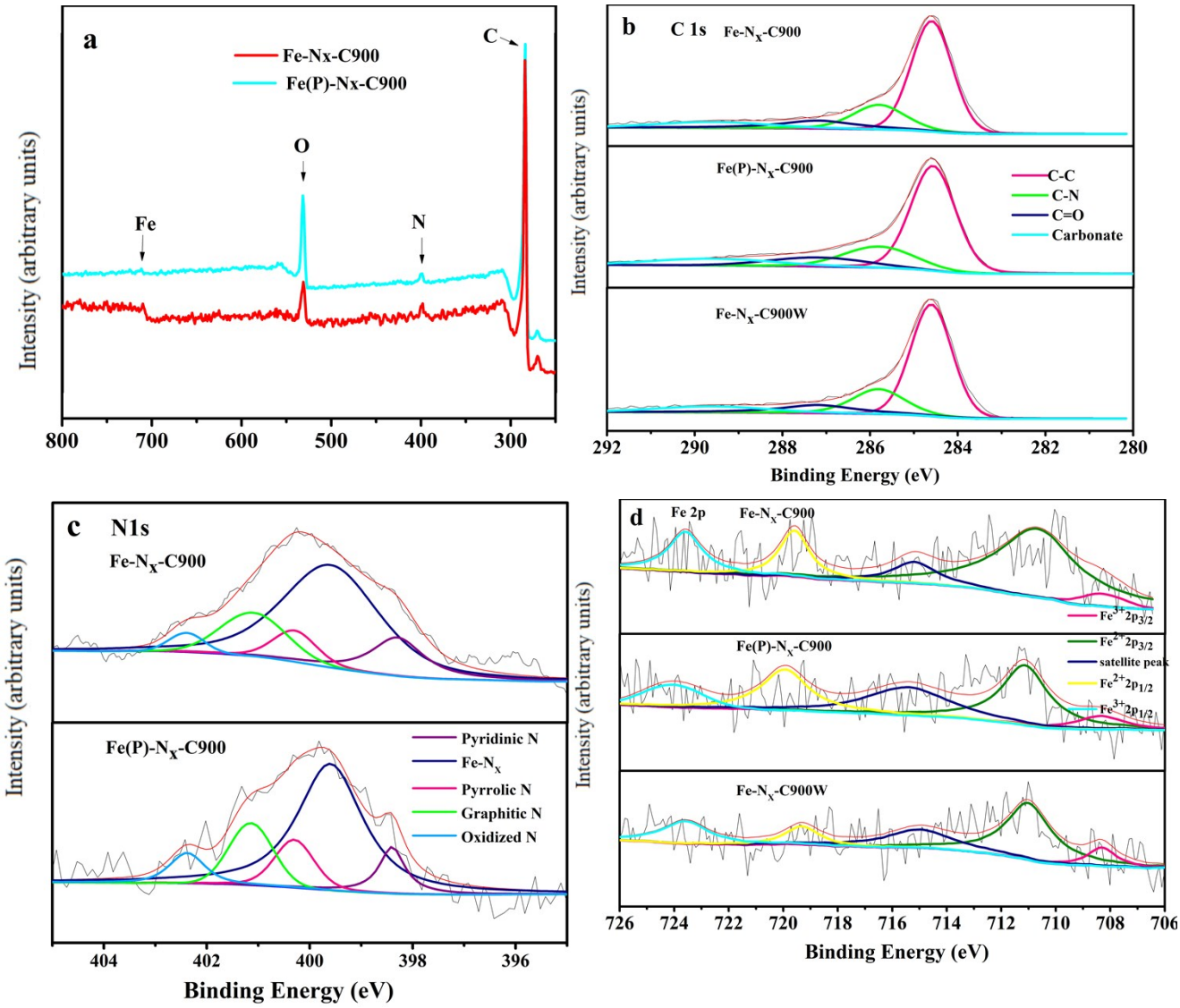

Fig. S3 (a) XPS survey spectra of Fe-N_x-C900 and Fe(P)-N_x-C900 (Pour Fe loading caused by multi-time washing after acid treatment), (b) N 1s and (c) C 1s spectra of Fe-N_x-C900 and Fe(P)-N_x-C900, and (d) Fe 2p spectra of Fe-N_x-C900AH, Fe(P)-N_x-C900 and Fe-N_x-C900W (Fe-N_x-C900W: acid-treated catalyst without 300 °C annealing in vaccum).

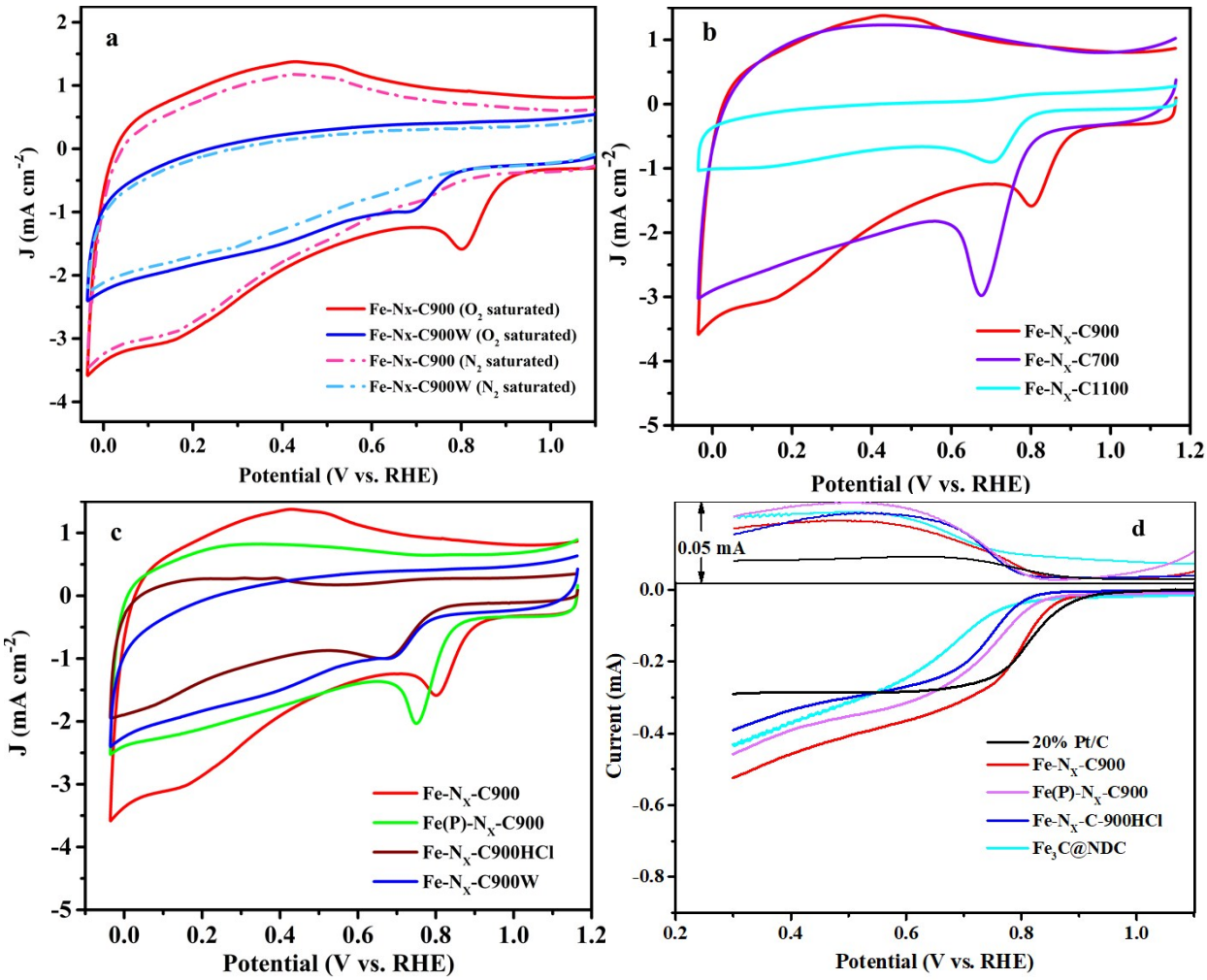

Fig. S4. (a) CV profile of the Fe-N_x-C900 and Fe-N_x-C900W in O_2 saturated or N_2 saturated 0.1M KOH, (b) CV profile of three catalysts in O_2 saturated 0.1M KOH at a scan rate of 50 mV s^{-1}, (c) CV profile of Fe-N_x-C catalysts in O_2 saturated 0.1M KOH at a scan rate of 50 mV s^{-1} (Fe(P)-N_x-C900: pour Fe loading catalyst caused by multi-time washing after acid treatment; Fe-N_x-C900HCl: catalyst is acid-treated by only HCl, leading to lots ferrous cores remains in the catalyst; Fe-N_x-C900W: acid-treated catalyst without 300 °C annealing in vaccum), and (d) RRDE of catalysts at a sweep rate of 10 mVs^{-1} under rotating speeds of 1600 rpm in O_2 saturated 0.1M KOH (Fe_3C@NDC, the precursor of Fe-N_x-C900 without acid treatment).

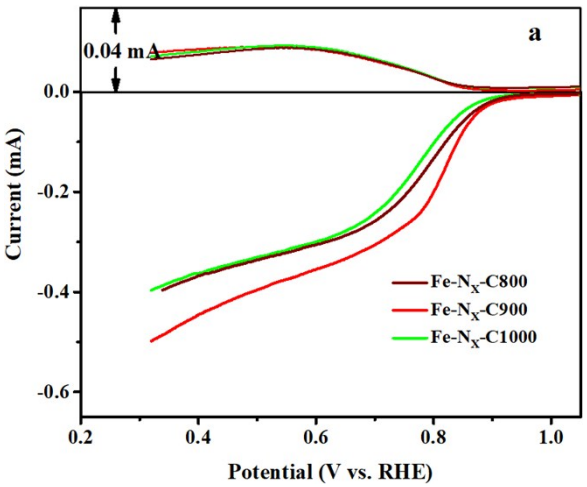

Fig. S5. (a) RRDE of catalysts at a sweep rate of 10 mVs^{-1} under rotating speeds of 1600 rpm in O_2 saturated 0.1M KOH

The transferred electron number (n) per oxygen molecule involved in ORR can be calculated by the currents measured from the ring and disk electrode in terms of the following equation:

$$n = \frac{4|i_d|}{|i_d| + i_r/N} \quad (1)$$

where N = 0.45, i_d and i_r are the collection efficiency, disk current and ring current, respectively.

The K-L plots has been calculated from the under K-L equation (2). The K–L plots show linear relationships between J_k^{-1} and $\omega^{-1/2}$ for Fe-N_x-C900 catalyst.

$$J^{-1} = J_K^{-1} + J_L^{-1} = J_K^{-1} + B^{-1}\omega^{-1/2} \quad (2)$$

$$B = 0.62nFC_O(D_O)^{2/3}\nu^{-1/6}$$

$$J_K = nFkC_O$$

where J is the measured current density; J_L is the diffusion limit current density; J_K is the dynamic current density; ω is the angular velocity of the disk (ω = 2πN, N is the linear rotation speed); n is the overall number of electrons transferred in oxygen reduction; F is

the Faraday constant; C_O is the bulk concentration of O_2; ν is the kinematic viscosity of the electrolyte, and k is the electron-transfer rate constant.

Table S1 characterization of reported novel Fe-N-C catalysts

Paper	Catalyst type	Fe (at.%)	S_{BET} (m^2 g^{-1})	Mesopore volume (cm^3 g^{-1})	E_{onset} (V)	$E_{1/2}$ (V)	J_K (mA cm^{-2})
[S1]	N-Fe-800	6.91	511.0	<0.44	0.96	0.82	5.3 at 0.5V
[S2]	NH_3-Fe-N-C-800	22.0(wt.%)	124.5	<0.4	0.939	0.869	-
[S3]	Fe-NMG	0.22	520.5	-	0.96	0.83	-
[S4]	Fe-N-C-800	0.08	775.5	-	0.965	0.83	-
[S5]	FNCT800–100	0.54	368.3	-	0.926	0.82	5.32 at 0.36V
[S6]	PVP-NaCl-Fe/N/C	0.34	414.5	-	-	0.878	-
[S7]	FeGH-ArNH3	5.4	338.5	-	0.936	0.84	5.4
[S8]	S-Fe/N/C	1.38	273.38	0.4929	0.911	0.799	5.05
[S9]	Fe@N/C-800	-	480.95	<1.523	0.92	0.81	-
In our work	Fe-N_x-C900	2.42	890	1.6	0.96	0.83	6.2 at 0.6V

[S1] B.L. Zhou, L.Z. Liu, P.W. Cai, G. Zeng, X.Q. Li, Z.H. Wen, L. Chen, Ferrocene-based porous organic polymer derived high-performance electrocatalysts for oxygen reduction, J. Mater. Chem. A 5 (2017) 22163-22169. https://doi.org/10.1039/c7ta06515a.

[S2] Z.J. Liu, J. Yu, X.Y. Li, L.X. Zhang, D. Luo, X.H. Liu, X.W. Liu, S.B. Liu, H.B. Feng, G.L. Wu, P.Z. Guo, H.L. Li, Z.H. Wang, X.S. Zhao, Facile synthesis of N-doped carbon layer encapsulated Fe_2N as an efficient catalyst for oxygen reduction reaction, Carbon 127 (2018) 636-642. https://doi.org/10.1016/j.carbon.2017.11.051.

[S3] M.M. Hossen, K. Artyushkova, P. Atanassov, A. Serov, Synthesis and characterization of high performing Fe-N-C catalyst for oxygen reduction reaction (ORR) in Alkaline Exchange Membrane Fuel Cells, Journal of Power Sources 375 (2018) 214-221. https://doi.org/10.1016/j.jpowsour.2017.08.036.

[S4] B.C. Liu, B.B. Huang, C. Lin, J.S. Ye, L.Z. OuYang, Porous carbon supported Fe-N-C composite as an efficient electrocatalyst for oxygen reduction reaction in alkaline and acidic media, Applied Surface Science 411 (2017) 487-493, https://doi.org/10.1016/j.apsusc.2017.03.150.

[S5] F. Tang, H.T. Lei, S.J. Wang, H.X. Wang, Z.X. Jin, A novel Fe-N-C catalyst for efficient oxygen reduction reaction based on polydopamine nanotubes, Nanoscale 9 (2017) 17364-17370. https://doi.org/10.1039/c7nr06844a.

[S6] W. Wang, J. Luo, H.W. Chen, J. Li, W. Xing, S.L. Chen, Mesoporous Fe/N/C oxygen reduction catalyst through NaCl crystallites-confined pyrolysis of polyvinylpyrrolidone, J. Mater. Chem. A. 4 (2016) 12768-12773. https://doi.org/10.1039/C6TA05075A.

[S7] M. Wang, Y.S. Yang, X.B. Liu, Z.H. Pu, Z.K. Kou, P.P. Zhu, S.C. Mu, The role of iron nitrides in the Fe-N-C catalysis system towards the oxygen reduction reaction, Nanoscale 9 (2017) 7641-7649. https://doi.org/10.1039/c7nr01925d.

[S8] K. Hu, L. Tao, D.D. Liu, J. Huo, S.Y. Wang, Sulfur-doped Fe/N/C nanosheets as highly-efficient electrocatalysts for oxygen reduction reaction. ACS Appl. Mater. Interfaces 8 (2016) 19379-19385. https://doi.org/10.1021/acsami.6b02078.

[S9] L. Zhang, C.L. Qi, A.H. Zhao, G.C. Xu, J.L. Xu, L. Zhang, C. Zhang, D.Z. Jia, N-doped porous carbon-encapsulated Fe nanoparticles as efficient electrocatalysts for oxygen reduction reaction, Applied Surface Science 445 (2018) 462-470. https://doi.org/10.1016/j.apsusc.2018.03.145.